Gourlay, T.P. 2009 Sinkage and trim of two ships passing each other on parallel courses. *Ocean Engineering* Vol. 36, No. 14, pp. 1119 – 1127.

Sinkage and trim of two ships passing each other on parallel courses

Tim Gourlay
Centre for Marine Science and Technology, Curtin University, Western Australia

Abstract

A theoretical method is used to predict the sinkage and trim of two moving ships as they pass each other, either from opposite directions, or as one ship overtaking the other. The description is simplified to open water of shallow constant depth. The method is based on linear superposition of slender-body shallow-water flow solutions. It is shown that even for head-on encounters, oscillatory heave and pitch effects are small, and sinkage and trim can be calculated using hydrostatic balancing. Results are compared to available experimental results, and applied to an example situation of a containership and bulk carrier in a head-on or overtaking encounter. Using dimensional analysis, simple approximate formulae are then developed for estimating the maximum sinkage of two similar vessels in a passing encounter.

1. Introduction

Passing manoeuvres of ships in shallow water can produce significant sway and yaw motions of each vessel, which can be dangerous if not properly understood and allowed for. Much research has been done into calculating these sway and yaw motions. Tuck & Newman (1974) developed a slender-ship method for calculating sway forces and yaw moments for two ships moving on parallel courses in deep water. The ships could each have arbitrary speeds, so the solution was valid for head-on encounters, overtaking manoeuvres, or for one ship stationary. King (1977) included the effect of horizontal circulation, applying a Kutta condition at each ship's stern. Yeung (1978) developed a shallow-water method, including the effect of circulation, to calculate sway forces and yaw moments on each ship. Davis & Geer (1982) developed an alternative method for calculating the slender-body sway forces and yaw moments, based on asymptotic analysis. Further numerical work to predict sway forces and yaw moments was done by Kijima (1987), while Brix (1993) developed expressions for the maximum sway forces and yaw moments during an overtaking manoeuvre. Calculated sway forces and yaw moments were used to define the limits of control during passing or overtaking manoeuvres in Xu et al (2008).

The specific problem of *vertical* motions of a moving ship, due to another passing ship, has received comparatively little attention. Yeung (1978) found analytically that the dominant heave force and pitch moment were due to linear superposition of the pressure fields produced by each ship. The circulation around each vessel, while important for sway forces and yaw moments, was found to have only a secondary effect on heave and pitch.

An experimental investigation into the transient sinkage and trim of passing model ships was undertaken by Dand (1981), involving the use of two independent towing carriages. These experiments showed the large changes in sinkage and trim that can occur for close passing manoeuvres, and the resulting increase in grounding risk.

In this article, we start with the theoretical basis developed by Yeung (1978) for two ships moving on parallel courses, and calculate sinkage and trim for example ships

through passing manoeuvres. Dimensional analysis will then be used to develop simple formulae for estimating the maximum sinkage of similar vessels during a passing manoeuvre.

2. Theoretical method

The slender-body shallow-water method is based on the theory of Tuck (1966) for a single ship. For simplicity we shall here consider the case of open water with constant depth, and assume the ships are passing on parallel courses from opposing directions. The ships are labelled “Base Ship” and “Passing Ship”. The geometry is shown in Figure 1, in the earth-fixed coordinates (x,y).

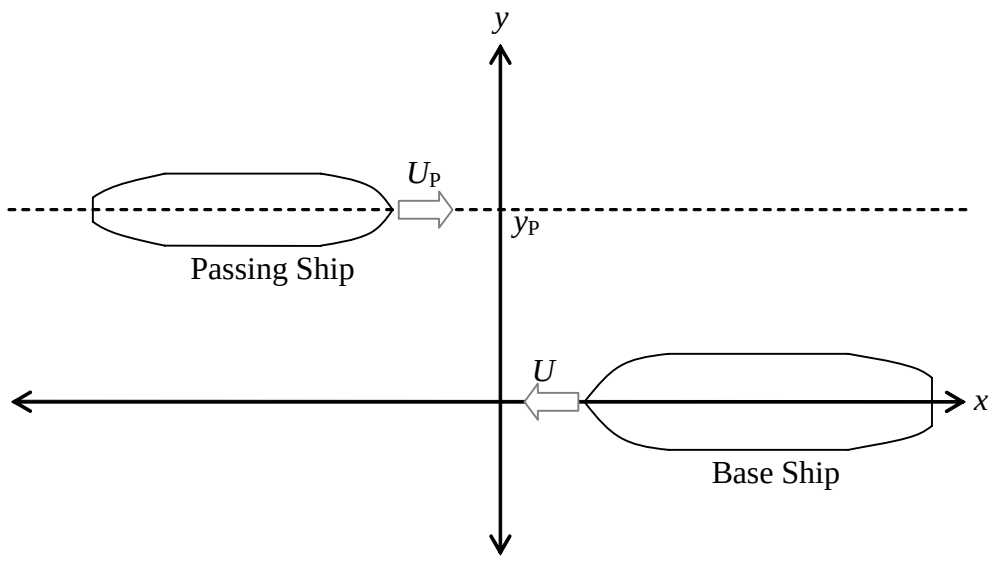

Figure 1: Coordinate system and notation

The y-coordinate is chosen such that the centreline of the base ship lies on $y = 0$, while the centreline of the passing ship lies on $y = y_P$. We assume that y_P is large compared to each ship’s beam, and of similar order to each ship’s length. In this way, each ship can be considered to lie entirely in the far field of the other vessel, as described in Yeung (1978).

The ship speeds U and U_P are assumed constant. As noted in the Dand (1981) experiments, head-on encounters and particularly overtaking encounters produce changes in resistance which translate into changes in ship speed at constant engine RPM. In this article however, this effect will not be included.

The “submerged length” of the base ship is L, which is the distance from the foremost part of the submerged hull (e.g. the front of the bulb, if present) to the aftmost part of the submerged hull. The submerged length is sometimes termed the “Length Overall Submerged” (L_{os}), but the subscripts will be omitted here, and the submerged length of the passing ship denoted L_P.

For mathematical convenience, “submerged midships” is midway between the foremost and aftmost points of the submerged hull on each ship. The (*x*,*t*) coordinates are chosen such that the submerged midships of both ships pass through $x = 0$ at time $t = 0$.

Following Tuck (1966), the hydrodynamic pressure field (pressure above hydrostatic) around the base ship can be written

$$p = -\frac{\rho U^2}{2\pi h\sqrt{1-F_h^2}} \int_{-L/2}^{L/2} \frac{S'(\xi)\left(X-\xi\right)}{\left(X-\xi\right)^2 + \left(1-F_h^2\right)y^2}\, d\xi \qquad (1)$$

Here *h* is the undisturbed water depth, assumed constant, and the depth-based Froude number is

$$F_h = \frac{U}{\sqrt{gh}} \qquad (2)$$

X is a ship-fixed coordinate centred on the ship’s submerged midships, with $X = x + Ut$ if the midships pass through $x = 0$ at time $t = 0$. $S(\xi)$ is the hull cross-sectional area at station ξ, with the forward extremity of the submerged hull at $\xi = -L/2$ and the aft extremity at $\xi = L/2$. The primed $S'(\xi)$ denotes the derivative $dS/d\xi$. The section area is calculated at the static floating position, since to leading order the pressure field is unaffected by the dynamic sinkage and trim of the ship.

Linear superposition of the pressure fields due to each ship, as proposed by Yeung (1978), yields the following expression for the pressure on the base ship:

$$\begin{aligned} p = &-\frac{\rho U^2}{2\pi h\sqrt{1-F_h^2}} \int_{-L/2}^{L/2} \frac{S'(\xi)}{X-\xi}\, d\xi \\ &-\frac{\rho U_P^2}{2\pi h\sqrt{1-F_P^2}} \int_{-L_P/2}^{L_P/2} \frac{-S_P'(\zeta)\left(X + X_{CC} + \zeta\right)}{\left(X + X_{CC} + \zeta\right)^2 + \left(1-F_P^2\right)y_P^2}\, d\zeta \end{aligned} \qquad (3)$$

The passing ship integral in the second term has $S_{\mathrm{P}}(\zeta)$ defined from the bow to the stern, as for the base ship, with the forward extremity at $\zeta = -L_P/2$ and aft extremity at $\zeta = L_P/2$. The depth-based Froude number of the passing ship is

$$F_{\mathrm{P}} = \frac{U_{\mathrm{P}}}{\sqrt{gh}} \qquad (4)$$

The pressure field is time-dependent, through the changing longitudinal distance between ship centres (positive when approaching)

$$X_{\mathrm{CC}} = -\left(U + U_{\mathrm{P}}\right)t \qquad (5)$$

The upwards vertical force *Z* on the base ship is found as in Tuck (1966) to be

$$Z = \int_{-L/2}^{L/2} p(X,t)\, B(X)\, dX \qquad (6)$$

while the bow-down trim moment about the LCF is

$$M_{\mathrm{LCF}} = \int_{-L/2}^{L/2} p(X,t)\,(X - X_{\mathrm{LCF}})B(X)\,dX \qquad (7)$$

3. Sinkage and trim

Equations (3,6,7) give the time-dependent vertical force and trim moment on the base ship. We now seek to determine sinkage and trim. The LCF sinkage s_{LCF} is defined as the sinkage of the LCF beneath its static floating position (i.e. positive downward), in metres when using SI units. The trim θ is defined as the *change* in trim (positive bow-down) as compared to the static floating position. This is calculated in radians according to the formulae, but will be plotted in degrees for clarity.

In order to determine sinkage and trim, we must first assess whether the flow changes are sufficiently rapid to cause oscillatory heave and pitch motions of the ship. A simple quasi-steady method to determine sinkage and trim assumes that forces remain more or less in equilibrium, in which case hydrostatic balancing can be used. In that case, the upwards vertical force *Z* is related to the quasi-steady sinkage s_{LCF} and waterplane area *A* through

$$Z = -\rho g A s_{\mathrm{LCF}} \qquad (8)$$

Similarly, M_{LCF} is related to the quasi-steady bow-down trim θ (in radians) through

$$M_{\mathrm{LCF}} = \rho g I_{\mathrm{LCF}} \theta \qquad (9)$$

$$I_{\mathrm{LCF}} = \int_{-L/2}^{L/2} (X - X_{\mathrm{LCF}})^2 B(X)\,dX \qquad (10)$$

However, if oscillatory heave and pitch are important, we need to use a seakeeping-type dynamic method to determine these. In calm water, if the LCF is close to the LCB, heave and pitch can be considered uncoupled (Bhattacharyya 1978). The sinkage equation of motion then follows the standard seakeeping form

$$(m + a_z)\frac{d^2 s_{\mathrm{LCF}}}{dt^2} + b_z \frac{ds_{\mathrm{LCF}}}{dt} + c_z s_{\mathrm{LCF}} = -Z(t) \qquad (11)$$

The “exciting force”, which in seakeeping problems would involve wave elevation terms, is the time-dependent downward vertical force $[-Z(t)]$. The coefficients are as follows:

m = ship mass
a_z = heave added mass
b_z = heave damping coefficient
c_z = heave restoring coefficient

According to strip theory, the coefficients are calculated by summing the contributions from each hull section. For example, the total added mass is

$$a_z = \int_{-L/2}^{L/2} a_n\,dX \qquad (12)$$

where a_n is the added mass per unit length of each hull cross-section. The other coefficients are calculated in a similar manner.

Again assuming the LCB is close to the LCF, the dynamic pitch equation (Bhattacharyya 1978) can be written

$$(I+\delta I)\frac{d^2\theta}{dt^2}+b_\theta\frac{d\theta}{dt}+c_\theta\theta=M_{\mathrm{LCF}}(t) \qquad (13)$$

The coefficients are as follows:

$$I=\int_{-L/2}^{L/2}(X-X_{\mathrm{LCF}})^2 m_n\,dX \qquad (14)$$

$$\delta I=\int_{-L/2}^{L/2}(X-X_{\mathrm{LCF}})^2 a_n\,dX \qquad (15)$$

$$b_\theta=\int_{-L/2}^{L/2}(X-X_{\mathrm{LCF}})^2 b_n\,dX \qquad (16)$$

$$c_\theta=\int_{-L/2}^{L/2}(X-X_{\mathrm{LCF}})^2 c_n\,dX \qquad (17)$$

In order to check the importance of dynamic heave and pitch, a numerical experiment was undertaken on two containerships passing each other. Both ships had S-175 standard series hull forms (ITTC 1987). A body plan for the S175 hull form is shown in Figure 2.

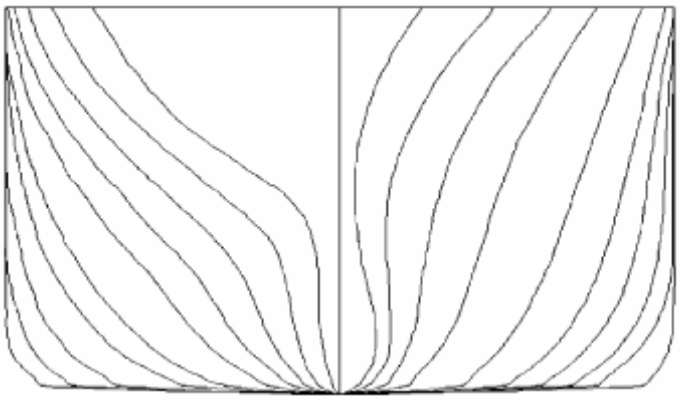

Figure 2: Body plan of S175 containership (Singh & Sen 2007)

Using a scaling factor of 1.268 from the original S175 design (ITTC 1987), the ship is scaled to a Panamax-size vessel as shown in Table 1.

Length between perpendiculars (L_{PP})	221.9m
Submerged forward extremity (front of bulb)	2.2m ahead of forward perpendicular
Submerged aft extremity (waterline)	4.1m behind aft perpendicular
Length overall submerged	228.2m
Beam	32.20m
Draft	12.05m
Static trim	Level
Displacement	49,210m^3 (50,450 tonnes)
LCB	1.4% L_{PP} aft of midships
LCF	4.0% L_{PP} aft of midships

Table 1: Details for sample containership

Note that the LCB and LCF are given relative to the conventional "midships", which is midway between the forward and aft perpendiculars.

Two ships with these dimensions were run past each other in a water depth h of 15.0m, at a passing distance y_P of 200m, with each ship travelling at 15 knots.

The dynamic coefficients used were representative values as shown in Table 2:

Coefficient	Value	Notes
m_n	ρS_n	Assuming ship mass evenly distributed according to section area
ω_e (representative encounter frequency)	$\frac{4\pi U}{L}$	Using representative encounter period taken from time of bows passing to time of sterns passing
a_n	m_n	Setting added mass equal to ship mass as representative value in shallow water
b_n	$\rho\omega_e B_n^2$	Low-frequency approximation from Bhattacharyya (1978) p44
c_n	$\rho g B_n$	from Bhattacharyya (1978) p47

Table 2: Dynamic coefficients used for numerical experiment

Once the time-dependent vertical force and trim moment had been calculated, the quasi-steady sinkage and trim were calculated directly from equations (8,9). The dynamic sinkage and trim were calculated from equations (11,13), using a standard ordinary differential equation solver in Matlab.

The calculated sinkage according to both methods is shown in Figure 3. The calculated trim from both methods is shown in Figure 4.

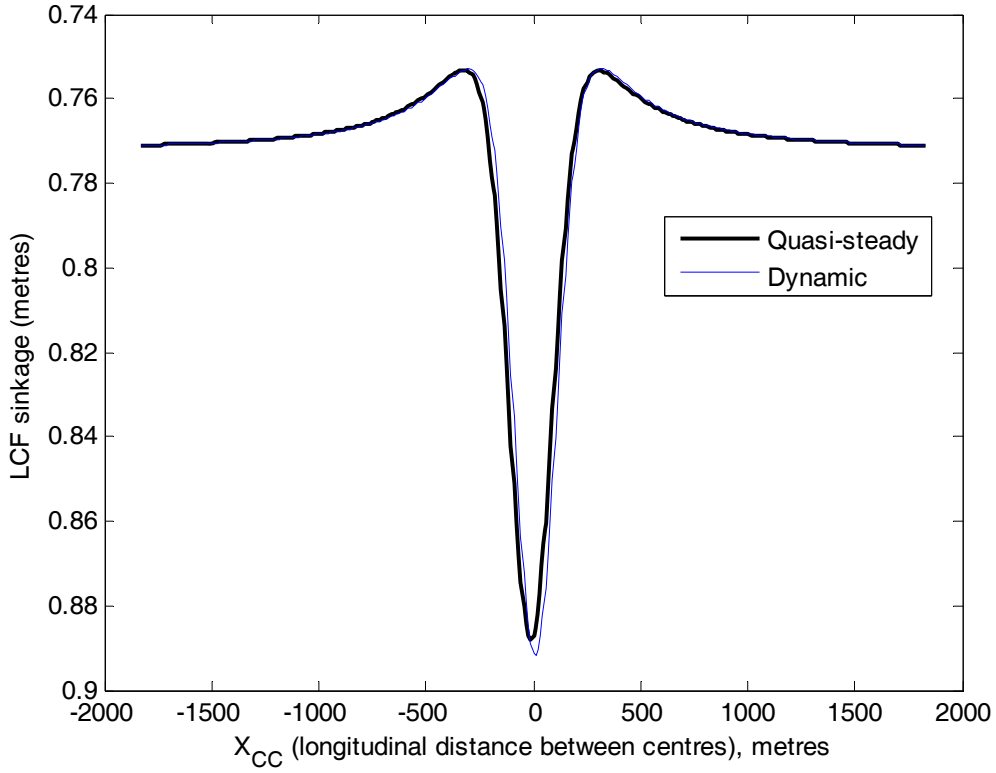

Figure 3: Calculated sinkage for numerical test case, according to quasi-steady and dynamic methods

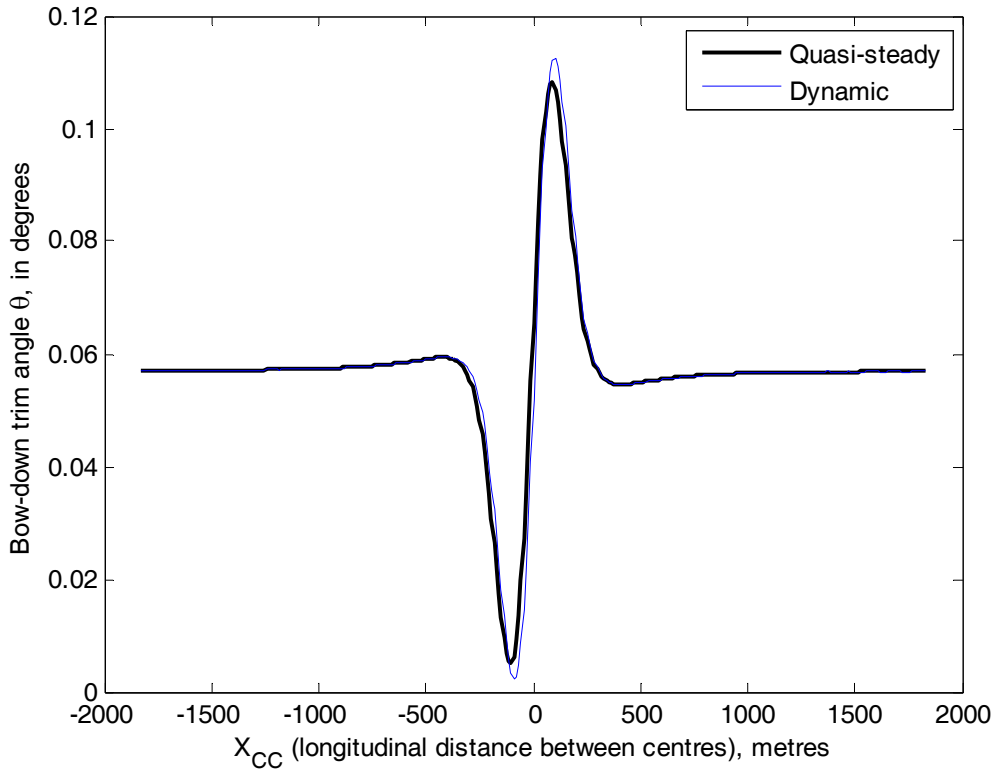

Figure 4: Calculated trim for numerical test case, according to quasi-steady and dynamic methods

These figures show the general form of the sinkage and trim, as two ships pass each other on opposing courses. Initially (large X_{CC}) the sinkage and trim are at their steady-state values. As the ships come closer together, the sinkage of each ship initially decreases, as the high pressure area ahead of each ship's bow causes a lesser downward force on the other ship. When the forward shoulders are in line ($X_{CC} \approx L/2$), the low pressure area around each ship's forward shoulders decreases the pressure on the other ship's forward shoulders, causing the trim to go more bow-down.

When the ships overlap ($X_{CC} \approx 0$), the low pressure areas along the forward and aft shoulders of each ship reinforce with those of the other ship, and the sinkage of both ships increases. When the ships' aft shoulders pass each other ($X_{CC} \approx -L/2$), the low pressure area around each ship's aft shoulders causes a lower pressure around the aft shoulders of the other ship, causing the trim to go more stern-down.

Regarding the comparison between the quasi-steady and dynamic methods, we see that both methods give very similar results for the predicted sinkage, and also for the predicted trim. Therefore it appears that the sinkage and trim of the ship are effectively in hydrostatic equilibrium during the entire passing manoeuvre, with the flow changing too slowly to produce dynamic heave and pitch oscillations. This test was done at quite a high speed (15 knots each ship), and close passing (y_P = 200m), given that the theory requires y_P to be of similar or greater order than the shiplength for the far-field assumption to be valid. When the numerical experiment was repeated for both ships travelling at slower speeds, or greater separation, the dynamic and quasi-steady methods were almost indistinguishable.

Looking at the time scales, it may be seen that the natural heave and pitch periods of a large containership or bulk carrier will typically be about 10 seconds in shallow water, while the time taken for two ships to pass each other will be in the order of 1 minute. Therefore the changes in vertical force and trim moment happen over a much longer time scale than the natural heave and pitch periods, giving the ship sufficient time to adjust its sinkage and trim and remain in hydrostatic equilibrium.

With this in mind, we henceforth use hydrostatic balancing to calculate sinkage and trim from the vertical force and trim moment, as in equations (8,9).

4. Bow and stern sinkage

While LCF sinkage (or midship sinkage) and dynamic trim remain the defining "raw results" of ship squat studies, the results that are of more importance in assessing grounding risk are the bow and stern sinkage, including the combined effects of LCF sinkage and dynamic trim.

In order to demonstrate the effect of passing manoeuvres on bow and stern sinkage, these have been calculated for the numerical test described in Section 3, using the quasi-steady method. Assuming a near-rigid hull, bow and stern sinkage follow geometrically from the LCF sinkage and dynamic trim results given in Figures 3 & 4.

Bow and stern sinkage for this test case are shown in Figure 5.

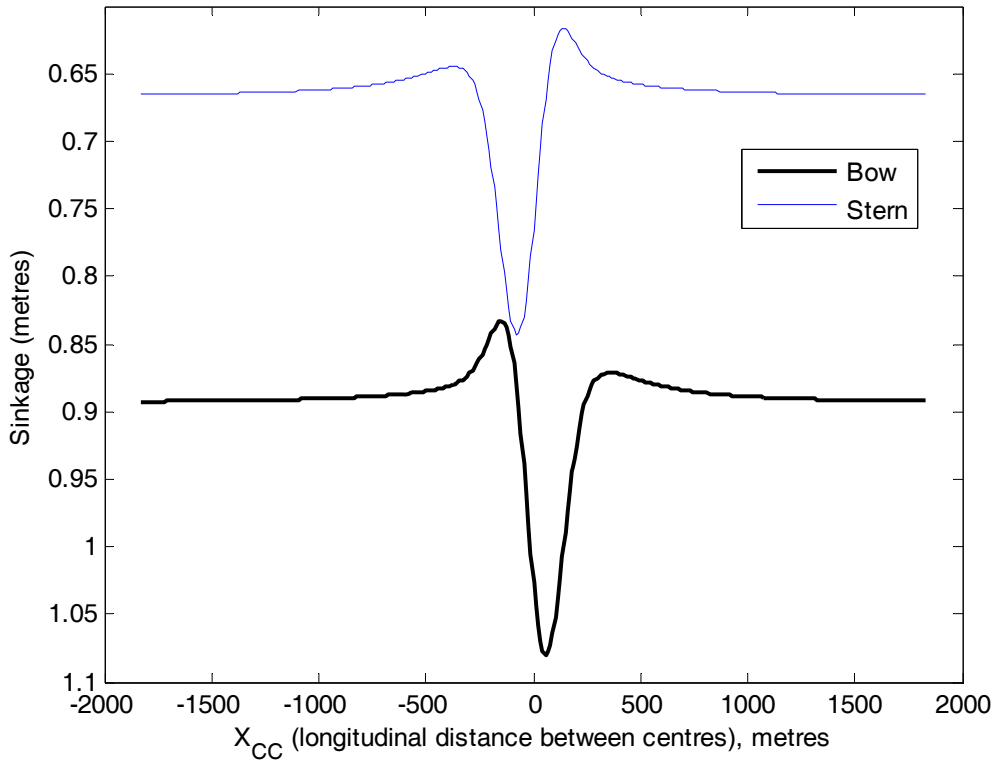

Figure 5: Bow and stern sinkage for test case described in Section 3

As discussed in Section 3, the defining effect on LCF sinkage is the large increase in LCF sinkage when the ships' midsections are in line. The defining effects on trim are the bow-down trim change when the forward shoulders are passing each other, and stern-down trim change when the aft shoulders are passing each other.

These effects translate clearly into bow and stern sinkage, as shown in Figure 5. Bow sinkage reaches a maximum just before the midships cross, while stern sinkage reaches a maximum just after the midships cross. The maximum increase above steady-state values is similar for both bow and stern sinkage, so the point on the ship most likely to ground will normally be that with the largest dynamic draft at steady state (in this case, the bow).

5. Comparison with experimental results

A brief comparison will now be made with experimental results from Dand (1981). This experimental study concentrated primarily on sway forces and yaw moments. Sinkage and trim results were presented as small-scale graphs, so that accurate comparison is only possible for limited cases. Therefore comparison with the Dand (1981) results is not sufficient to validate the theory, but a comparison is included here for completeness, since these are the only experimental results available.

The experiments used two different general cargo vessels, for which lines plans were provided. The results reproduced here are from Fig. 19 of that report, for the largest sinkage case where $F_h = 0.369$ and $F_{\mathrm{P}} = 0.422$. The length between perpendiculars

of the base ship is 3.96m, while that of the passing ship is 3.32m. The passing distance between centres is $y_p / B = 1.59$. Note that this violates the far-field assumption described in Section 2, as it is a very close-passing manoeuvre. However it was the only case for which the results were sufficiently legible to be reproduced.

Because of the small scale of the graphs, and uncertainty in the actual non-dimensionalization used, only results for midship sinkage are reproduced, and these have been scaled against the steady-state values. Results are shown in Figure 6. The error involved in reading the graphs given in the report is estimated at 10% because of their small scale.

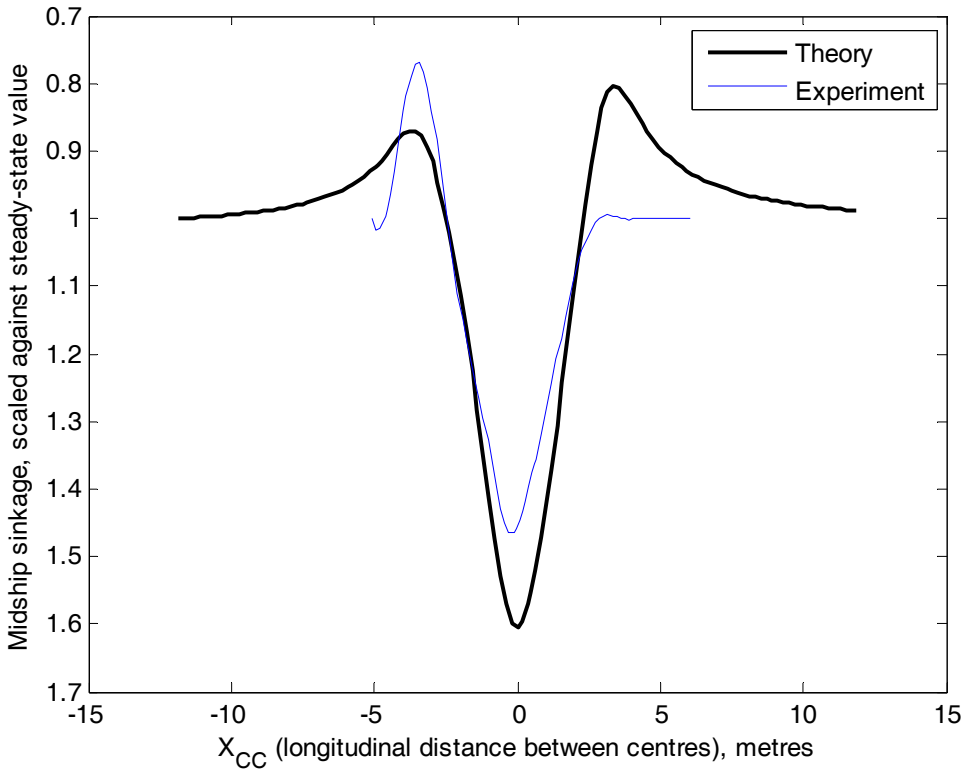

Figure 6: Midship sinkage, scaled against steady-state value, according to Dand (1981) experiments. Theoretical predictions for the same case also shown.

We see that for this case the maximum midship sinkage is reasonably well predicted, while the predicted decrease in midship sinkage when the ships were bow-to-bow and stern-to-stern was different in the experimental results.

As stated previously, these comparisons are of limited usefulness, since the close separation used for the experiments lies outside the range of validity of the slender-body method, and the error involved with reading the small-scale graphs was estimated at 10%. It is hoped that in future more experimental results will become available, with which to test the theory more closely.

6. Sample results for containership and bulk carrier

Here we present some sample results from the theoretical method, for the case of a containership and bulk carrier passing from opposing directions. The containership is a S-175 standard series (ITTC 1987), with hull details given in Table 1. The bulk carrier is a Japan Ship Research Institute 1704B standard series (Yokoo 1966) at full load. The bulk carrier is scaled to the dimensions shown in Table 3.

Length between perpendiculars (L_{PP})	240.0m
Submerged forward extremity (front of bulb)	6.2m ahead of forward perpendicular
Submerged aft extremity (waterline)	6.0m behind aft perpendicular
Length overall submerged	252.2m
Beam	36.92m
Draft	13.36m
Static trim	Level
Displacement	94,980m^3 (97,350 tonnes)
LCB	2.6% L_{PP} forward of midships
LCF	0.3% L_{PP} aft of midships

Table 3: Details for sample bulk carrier

The containership is travelling at 15 knots, while the bulk carrier is travelling at 10 knots. The water depth is 15.0m. Figures 7 & 8 give the sinkage of the containership and bulk carrier, for a range of passing distances y_P.

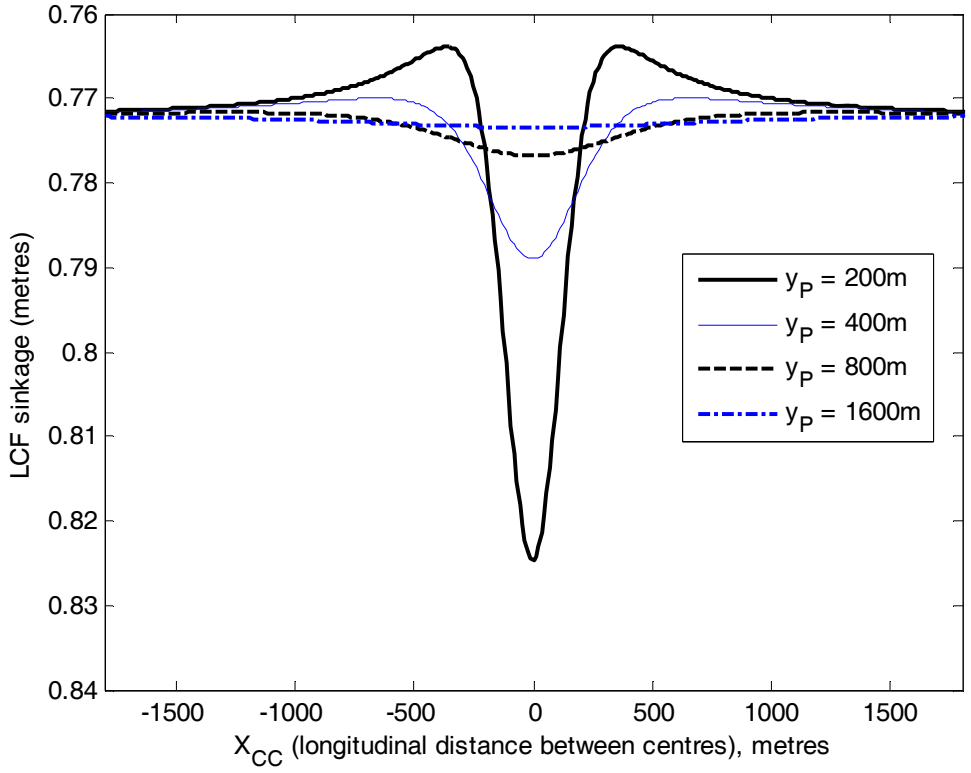

Figure 7: LCF sinkage for containership, travelling at 15 knots

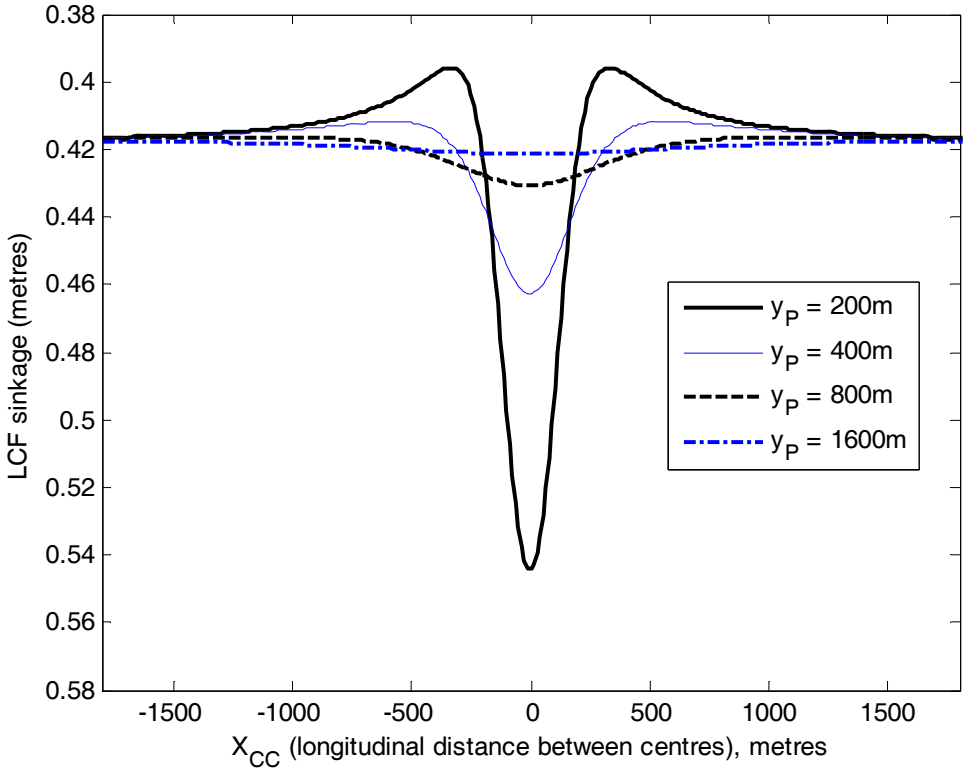

Figure 8: LCF sinkage for bulk carrier, travelling at 10 knots

These figures show the following:

- The effect of the passing ship is greatly reduced as the separation increases. At a separation of 800m, there is only a small effect from each ship on the other.
- Because of its larger speed, the containership causes more disturbance to the surrounding water than the bulk carrier does. Hence the containership has a larger effect on the bulk carrier than the bulk carrier has on the containership.

Figures 9 & 10 give the trim of the containership and bulk carrier, for a range of passing distances y_P.

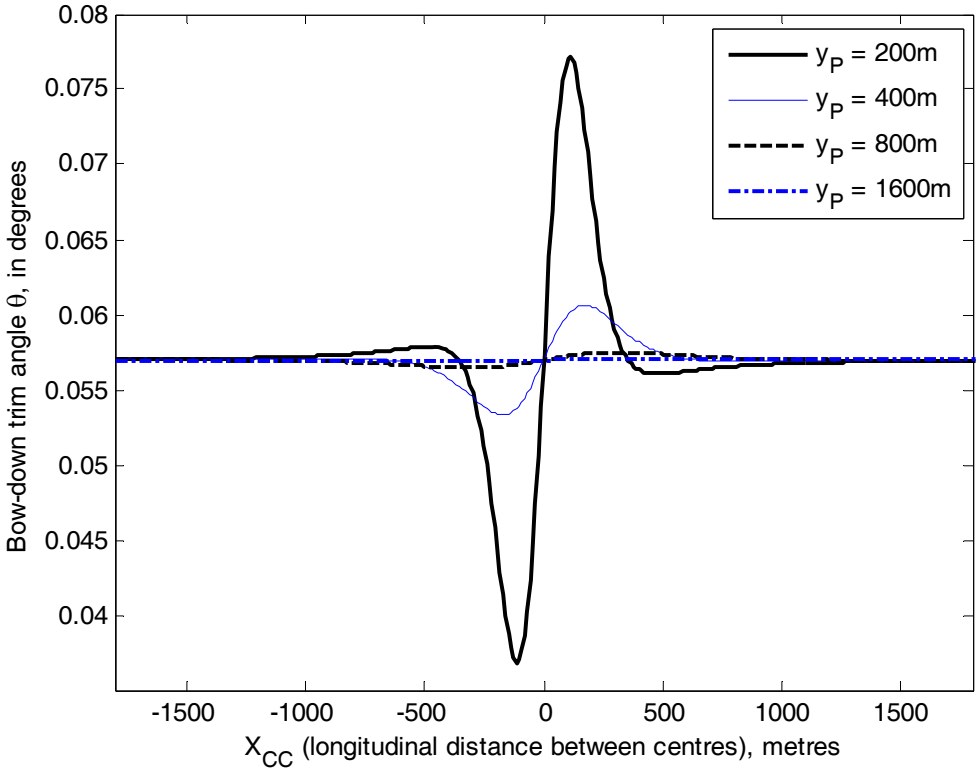

Figure 9: Trim angle for containership, travelling at 15 knots

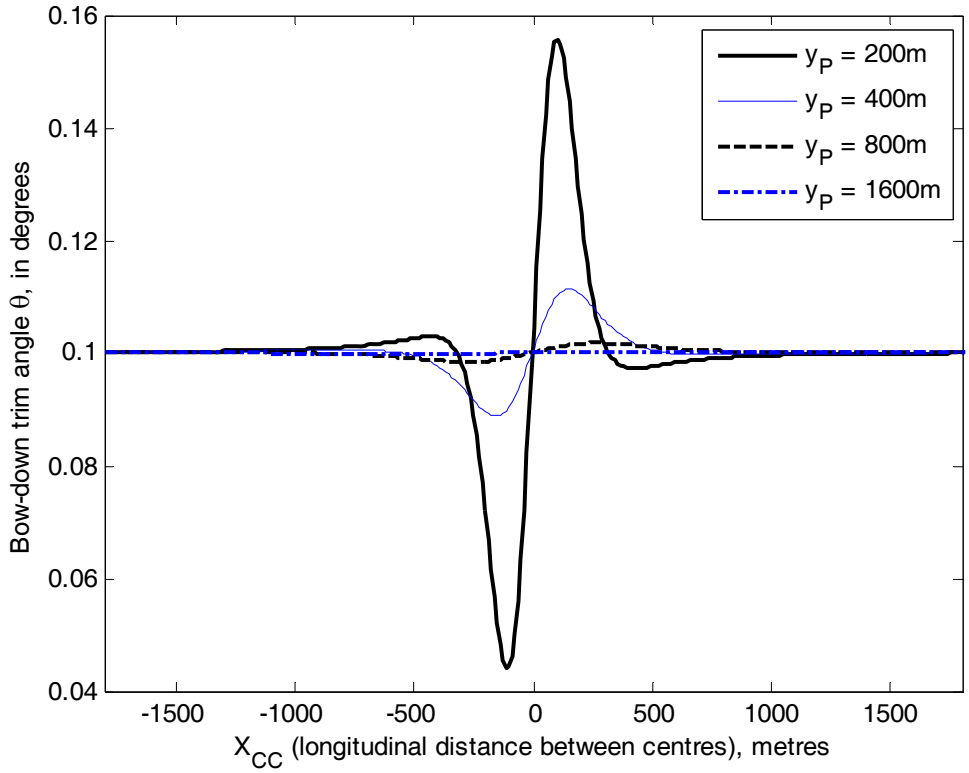

Figure 10: Trim angle for bulk carrier, travelling at 10 knots

The effect on both ships is for a bow-down trim change when the forward shoulders are passing each other, and stern-down trim change when the aft shoulders are passing

each other. As with sinkage, we see that the containership has a larger effect on the bulk carrier than vice versa.

7. Overtaking manoeuvres

For overtaking manoeuvres on parallel courses, we take both ships to be travelling in the negative x-direction, such that the midships of both ships pass through $x = 0$ at time $t = 0$. This situation is shown in Figure 11.

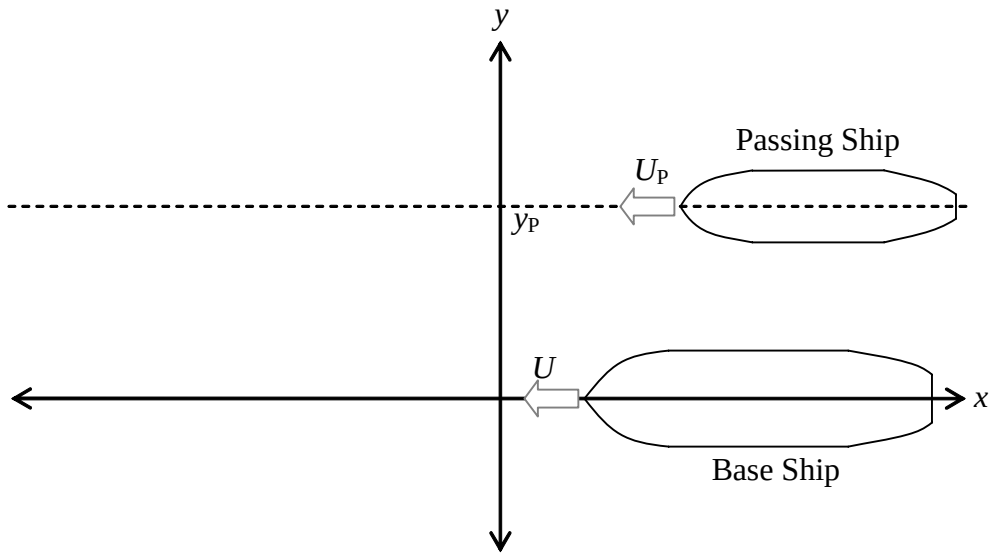

Figure 11: Coordinate system for overtaking manoeuvre

The total pressure field acting on the base ship is in this case

$$p = -\frac{\rho U^2}{2\pi h\sqrt{1-F_h^2}}\int_{-L/2}^{L/2}\frac{S'(\xi)}{X-\xi}d\xi - \frac{\rho U_P^2}{2\pi h\sqrt{1-F_P^2}}\int_{-L_P/2}^{L_P/2}\frac{S_P'(\zeta)\left(X-X_{CC}-\zeta\right)}{\left(X-X_{CC}-\zeta\right)^2+\left(1-F_P^2\right)y_P^2}d\zeta \qquad (18)$$

As for the passing ship case, X_{CC} is defined as the longitudinal distance between ship centres (positive when approaching), which is given by

$$X_{CC} = -\left(U_P - U\right)t \qquad (19)$$

Since the flow due to each ship is port-starboard symmetric, equations (18,19) apply equally to ships overtaking on the port or starboard side. The same equations (18,19) can also be used to find the pressure acting on the overtaking ship, by swapping the ship hulls (giving $U_P < U$) and reversing the sign of X_{CC} in equations (18,19), so that X_{CC} is still defined as being positive when the ships are approaching.

For ships passing from opposing directions, it was shown that flow changes are sufficiently gradual that the quasi-steady method is adequate for evaluating sinkage and trim. For overtaking manoeuvres, changes in sinkage and trim happen even more slowly, so we may use the quasi-steady method for this case also.

As an illustration of this method, consider the containership described in Table 1, travelling at 15 knots and overtaking the bulk carrier described in Table 3, travelling at 10 knots. The water depth is again 15.0m. Sinkage and trim of both vessels were calculated for this case using equations (18,19,6,7,8,9). The results are shown in Figures 12 – 15. In each case X_{CC} is positive when the ships are approaching.

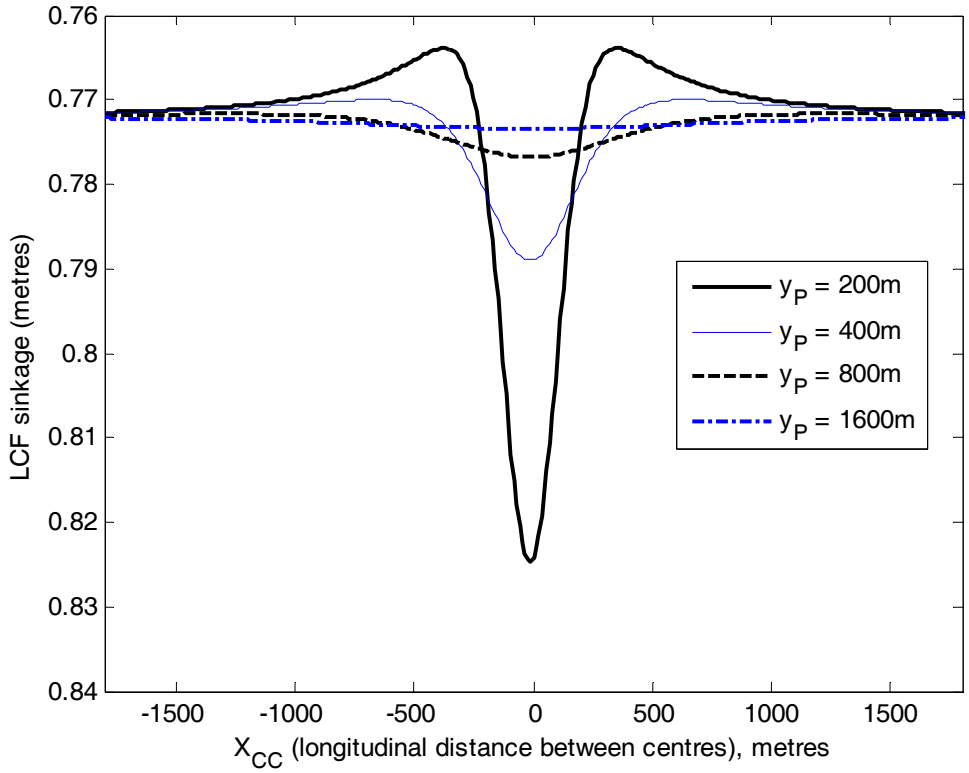

Figure 12: LCF sinkage of containership, as it overtakes the bulk carrier

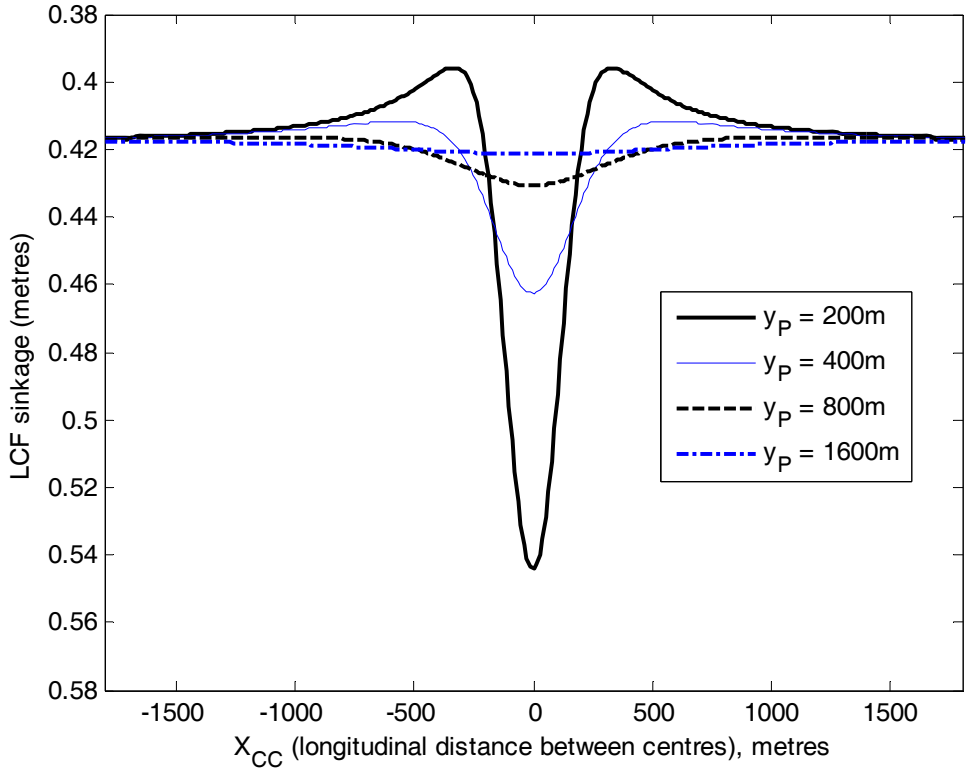

Figure 13: LCF sinkage of bulk carrier, as it is overtaken by the containership

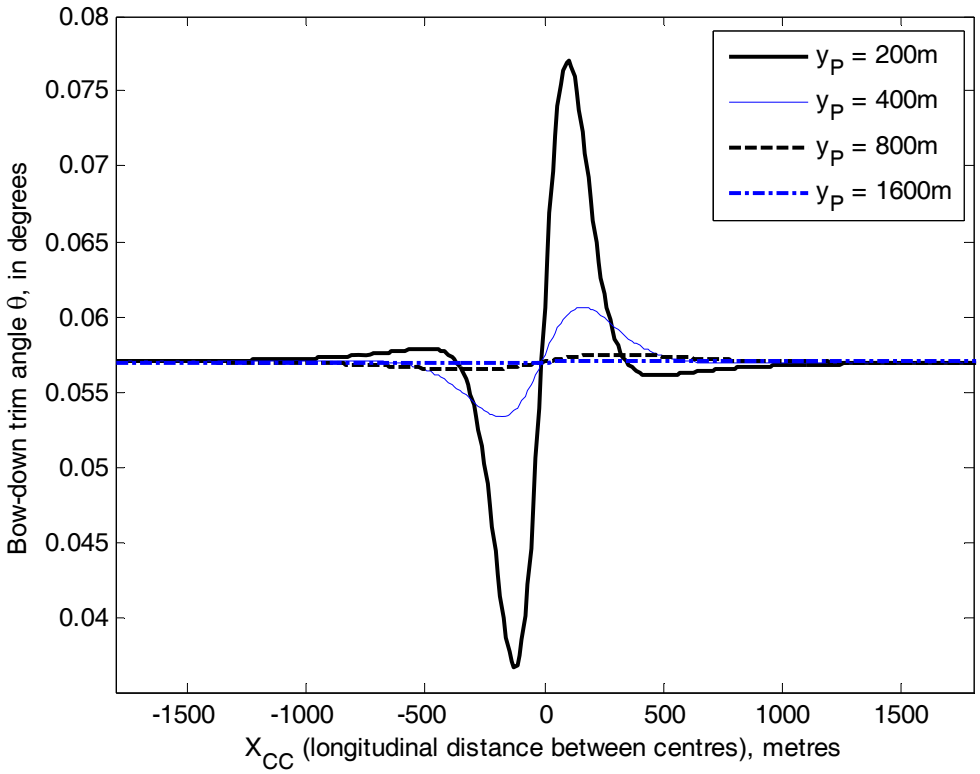

Figure 14: Trim of containership, as it overtakes the bulk carrier

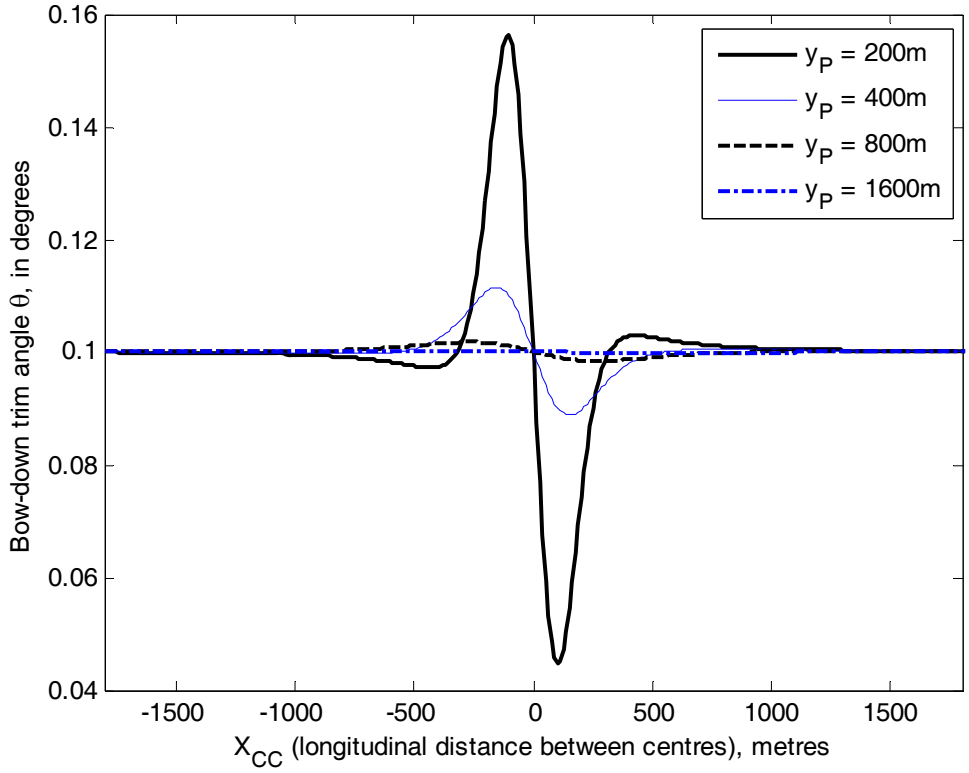

Figure 15: Trim of bulk carrier, as it is overtaken by the containership

We see that the graphs are related to those shown in Figures 7 – 10, for the same ships passing from opposing directions. As the bow of the containership approaches the stern of the bulk carrier, the sinkage of each vessel initially decreases, as the high pressure region near the bow and stern of each vessel decreases the sinkage force on the other vessel. When the forward shoulders of the containership reach the aft shoulders of the bulk carrier ($X_{CC} \approx L/2$), the low pressure region around the bulk carrier's aft shoulders decreases the pressure on the containership's forward shoulders, causing its trim to go more bow-down. At the same time, the low pressure region around the containership's forward shoulders decreases the pressure on the bulk carrier's aft shoulders, causing its trim to go more stern down.

Similarly, once the aft shoulders of the containership reach the forward shoulders of the bulk carrier ($X_{CC} \approx -L/2$), the combined low pressure fields cause the containership's trim to go more stern-down, and the bulk carrier's trim to go more bow-down. While the ships overlap ($X_{CC} \approx 0$), the dominating effect is an increase in midship sinkage of both vessels, as for the head-on encounter.

Importantly, the maximum trim and LCF sinkage are similar during the overtaking manoeuvre and head-on encounter at the same ship speeds.

8. Simplification of the formulae

8.1 Head-on encounters

In terms of under-keel clearance, the most important output from the analysis is the maximum sinkage during a passing manoeuvre. Using dimensional analysis, simple expressions for maximum sinkage may be obtained in certain cases. Noting that the LCF sinkage is proportional to the vertical force *Z*, we write equation (6) in the form

$$Z = -\frac{\rho U^2}{2\pi h\sqrt{1-F_h^2}} \int_{-L/2}^{L/2} \int_{-L/2}^{L/2} \frac{S'(\xi)B(X)}{X-\xi} d\xi\, dX \cdot \left\{ 1 + \left[\frac{U_P^2\sqrt{1-F_h^2}}{U^2\sqrt{1-F_P^2}} \frac{\int_{-L/2}^{L/2} \int_{-L_P/2}^{L_P/2} \frac{-S_P'(\zeta)\left(X+X_{CC}+\zeta\right)B(X)}{\left(X+X_{CC}+\zeta\right)^2+\left(1-F_P^2\right)y_P^2} d\zeta\, dX}{\int_{-L/2}^{L/2} \int_{-L/2}^{L/2} \frac{S'(\xi)B(X)}{X-\xi} d\xi\, dX} \right] \right\} \quad \textbf{(20)}$$

The term in square brackets is the fractional increase in sinkage force, and hence LCF sinkage, due to the passing vessel. The maximum sinkage is found by maximizing this function over longitudinal separation X_{CC}. An attempt was made to simplify this expression for general hull shapes using dimensional analysis, however it was found that the solution was too sensitive to the differing section area distribution of each hull, and had a complex dependence on the ratio between ship lengths. A similar conclusion was drawn by Dand (1981) when attempting to find empirical expressions for the maximum sinkage of different hulls, based on experimental results.

For the special case of identical hulls with differing speeds, we write the maximum LCF sinkage as

$$s_{\text{LCF.max}} = (1+\varepsilon_{\text{LCF}})\, s_{\text{LCF.steady}} \quad \textbf{(21)}$$

where, using equation (20)

$$\varepsilon_{\text{LCF}} = \frac{U_P^2\sqrt{1-F_h^2}}{U^2\sqrt{1-F_P^2}}\, f_{\text{LCF}}\left(\frac{y_P\sqrt{1-F_P^2}}{L} \right) \quad \textbf{(22)}$$

The function f_{LCF} might also depend on the non-dimensional hull shape, however this dependence is very weak, as we shall see. The function f_{LCF} was calculated for the cases of two container ships with details as shown in Table 1, and two bulk carriers with details as shown in Table 3. In each case the base ship was given a speed of 10 knots, while the passing ship had speeds ranging between 5 and 15 knots. The passing distances ranged between 0.5 and 4 times the Length Overall Submerged. Results are shown in Figure 16.

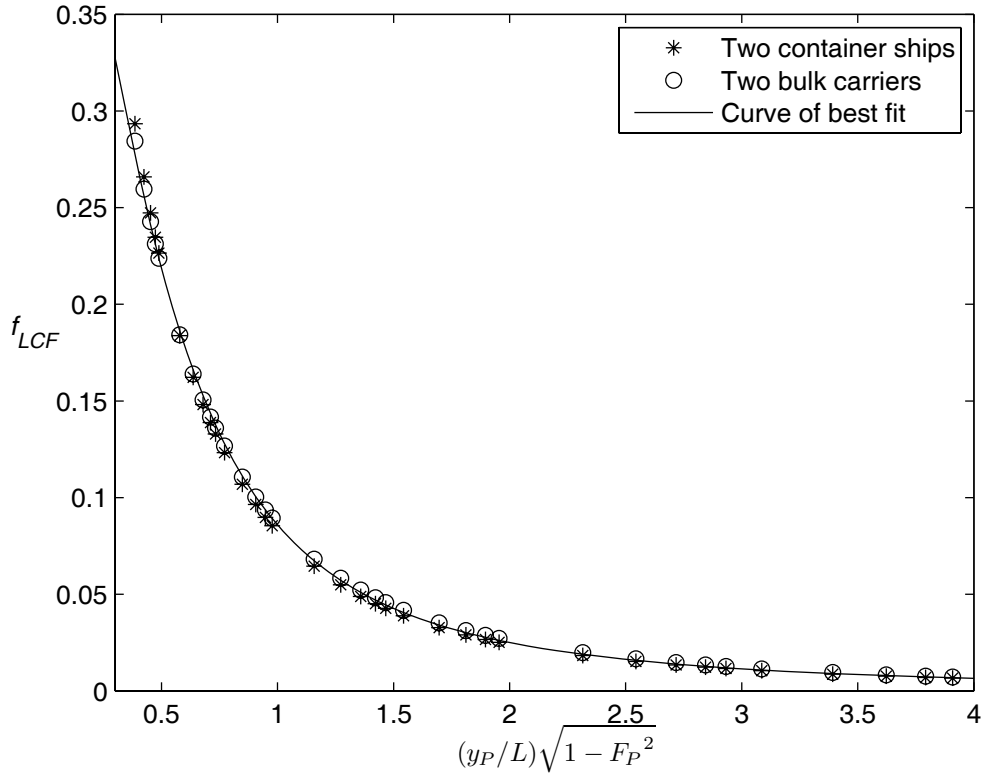

Figure 16: Scaled maximum increase in LCF sinkage due to a passing vessel of similar hull shape

Also shown in Figure 16 is a line of best fit to the function *f*, using the formulation suggested by equation (20)

$$f_{\mathrm{LCF}}(\eta) = \frac{1}{a_1 + a_2\eta^2} \qquad \textbf{(23)}$$

It is seen that despite the vastly different hull forms of the container ship and bulk carrier, the function *f* is almost identical in each case. Also, the function is well approximated using the functional form suggested in equation (23), with least-squares fit

$$f_{\mathrm{LCF}}(\eta) = \frac{1}{2.2 + 9.4\eta^2} \qquad \textbf{(24)}$$

The maximum bow and stern sinkage can be non-dimensionalized in a similar fashion, though these are best scaled against the LCF sinkage, due to the dynamic trim sensitivity with longitudinal volume distribution. The expressions used are

$$\begin{aligned} s_{\mathrm{bow.max}} &= s_{\mathrm{bow.steady}} + \varepsilon_{\mathrm{bow}}\, s_{\mathrm{LCF.steady}} \\ s_{\mathrm{stern.max}} &= s_{\mathrm{stern.steady}} + \varepsilon_{\mathrm{stern}}\, s_{\mathrm{LCF.steady}} \end{aligned} \qquad \textbf{(25)}$$

$$\begin{aligned} \varepsilon_{\mathrm{bow}} &= \frac{U_P^2\sqrt{1-F_h^2}}{U^2\sqrt{1-F_P^2}}\, f_{\mathrm{bow}}\left(\frac{y_P\sqrt{1-F_P^2}}{L}\right) \\ \varepsilon_{\mathrm{stern}} &= \frac{U_P^2\sqrt{1-F_h^2}}{U^2\sqrt{1-F_P^2}}\, f_{\mathrm{stern}}\left(\frac{y_P\sqrt{1-F_P^2}}{L}\right) \end{aligned} \qquad \textbf{(26)}$$

The calculated functional values for the above case are shown in Figures 17 and 18 for the bow and stern sinkage, together with curves of best fit.

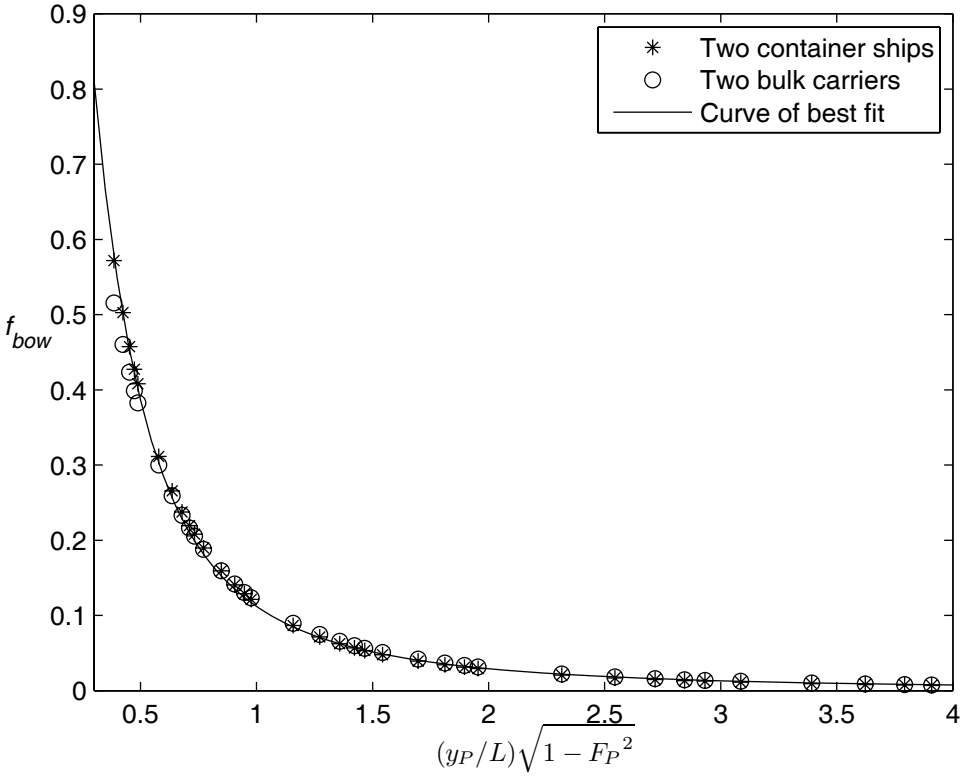

Figure 17: Scaled maximum increase in bow sinkage due to a passing vessel of similar hull shape

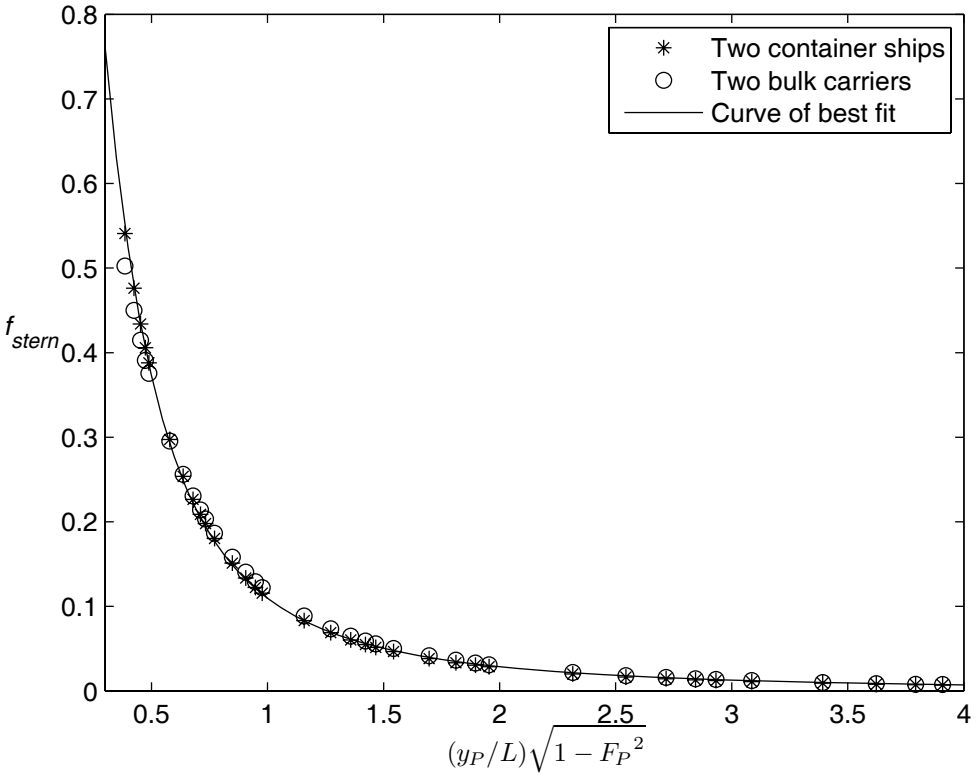

Figure 18: Scaled maximum increase in stern sinkage due to a passing vessel of similar hull shape

Again, the data collapse onto single curves despite the very different hull shapes. The least-squares curve fits are

$$f_{\text{bow}}(\eta) = \frac{1}{0.5 + 8.5\eta^2}$$
$$f_{\text{stern}}(\eta) = \frac{1}{0.5 + 8.6\eta^2} \qquad (27)$$

8.2 Overtaking encounters

Overtaking encounters were analyzed for the same ships and passing distances described in Section 8.1. The slower ship was given a speed of 4 knots, while the overtaking ship had speeds ranging from 5 to 15 knots. The dimensionless results were indistinguishable from the graphs in Figures 16 – 18, and the functional forms given in equations 21 – 27 were found to be equally applicable to overtaking encounters.

This follows the results of Section 7, in which it was seen that the maximum sinkage experienced by each ship during an overtaking manoeuvre is very similar to that which would be experienced in a head-on encounter at the same ship speeds.

8. Conclusions

A theoretical method based on that of Yeung (1978) has been described for predicting the sinkage and trim of two ships passing each other in head-on or overtaking

encounters. It was shown that even for high relative ship speeds, the vertical forces remain essentially in equilibrium, and sinkage and trim can be calculated by hydrostatic balancing.

Comparison was made between the numerical predictions and the experimental results of Dand (1981), showing reasonable agreement. Further experimental data to check the theory against would be desirable.

Sample numerical results have been presented for the case of a containership and bulk carrier passing each other from opposing directions. It was seen that the main qualitative effects are a bow-down change in trim when the forward shoulders pass each other, an increase in LCF sinkage when the midships pass each other, and a stern-down change in trim when the aft shoulders pass each other. These effects are diluted as the lateral distance between centres increases.

The theory was extended to calculate the sinkage and trim of two ships during an overtaking manoeuvre. Numerical calculations showed that the maximum bow, stern and LCF sinkage in this case are very similar to the case of ships passing from opposing directions.

For the special case of two identical ships passing in a head-on or overtaking encounter, a simple approximate method to predict the maximum sinkage was found using dimensional analysis.

This article described the case of two ships passing in open water of constant depth. For ships passing in dredged channels or canals of reasonable width, the single-ship flow fields given in Gourlay (2008) can be linearly superposed to describe the total flow around two ships travelling on parallel courses, as is done in this article for open water. This will then allow the sinkage and trim of each vessel to be calculated for that particular channel geometry.

9. References

Bhattacharyya, R. 1978 Dynamics of Marine Vehicles. Wiley Series in Ocean Engineering.

Brix, J. 1993 Maneuvering Technical Manual. Seehafen Verlag GmbH, Hamburg.

Dand, I.W. 1981 Some measurements in interaction between ship models passing on parallel courses. National Maritime Institute Report 108.

Davis, A.M.J. & Geer, J.F. 1982 The application of uniform-slender-body theory to the motion of two ships in shallow water. Journal of Fluid Mechanics 114, 419 – 441.

Gourlay, T.P. 2008 Slender-Body Methods for Predicting Ship Squat. Ocean Engineering 35(2), 191 – 200.

ITTC 1987 Report of the seakeeping committee, S-175 comparative model experiments. Proc. 18th International Towing Tank Conference (ITTC), Vol. 1, Kobe, Japan.

Kijima, K. 1987 Maneuverability of ships in confined water. International Conference of Ship Maneuverability, London.

King, G.W. 1977 Unsteady hydrodynamic interactions between ships. Journal of Ship Research 21, 157 – 164.

Singh, S.P. & Sen, D. 2007 A comparative study on 3D wave load and pressure computations for different level of modelling of nonlinearities. Marine Structures 20(1), 1 – 24.

Tuck, E.O. 1966 Shallow water flows past slender bodies. Journal of Fluid Mechanics 26, 81 – 95.

Tuck, E.O. & Newman, J.N. 1974 Hydrodynamic interaction between ships. 10th Symposium on Naval Hydrodynamics. Cambridge, Mass., 35 – 58.

Xu, Y., Zoub, Z., Liua, M. & Varyani, K.S. 2008 Study on critical-uncontrollable hydrodynamic interaction between ships. Proc. 18th International Offshore and Polar Engineering Conference, Vancouver, Canada.

Yeung, R.W. 1978 On the interaction of slender ships in shallow water. Journal of Fluid Mechanics 85, 143 – 159.

Yokoo, K. 1966 Systematic series model tests in Japan concerning the propulsive performance of full ship forms. Japan Shipbuilding and Marine Engineering, May 1966.